ORIENTAL JOURNAL OF CHEMISTRY
An International Open Access, Peer Reviewed Research Journal
www.orientjchem.org
ISSN: 0970-020 X
CODEN: OJCHEG
2026, Vol. 42, No.(5):
Pg. 1962-1973

Design and Synthesis of Novel Pyrazole-sulfonamide Derivatives as Dual Anti-inflammatory and Antioxidant Agents

VIJAY SHARMA[1], PANKAJ PRADHAN[2], YOGESH KR SHARMA[3], DEEKSHA VERMA[4], RAJEEV KUMAR SHARMA[5], RAJESH KUMAR[6], ANITA D. KADAM[7], RASHMI SHARMA[8] and CHETAN GHULAXE[9]*

[1]Professor, Pharmacy Academy, Faculty of Pharmacy, IFTM University, Moradabad UP.
[2]Professor, Swami Keshvanand Institute of Pharmacy, Ramnagaria, Jagatpura, Jaipur.
[3]Principal, Maharaja agrasen college of pharmacy nagar, Deeg, Bharatpur, Rajasthan.
[4]Assistant Professor, Teerthanker Mahaveer College of Pharmacy,
Teerthanker Mahaveer University Moradabad-244001, Uttar Pradesh, India.
[5]Associate Professor,DIT University Faculty of Pharmacy ,Mussorie Diversion Road Village
Makkawala PO Bhagwantpur,Dehradun Uttarakhand.
[6]Research Scholar, Apex university, Jaipur; Email: jatchaudhary088@gmail.com
[7]Tutor, Department of Biochemistry , Symbiosis Medical College for Women, Symbiosis
International (Deemed University), Pune,, Maharashtra, India.
[8]Assistant professor, Shri vaishnav institute of paramedical sciences, Shri vaishnav vidyapeeth
vishwavidyalaya, Indore-Ujjain Road , Gram Baroli, Indore, Madhya Pradesh - 453111.
[9]Assistant Professor, P. R. Patil Institute of Pharmacy, Talegaon (SP),
Dist. Wardha, Maharashtra 442202.
*Corresponding author E-mail: chetanghulaxe@gmail.com

http://dx.doi.org/10.13005/ojc/420516

(Received: April 22, 2026; Accepted: September 02, 2026)

ABSTRACT

The relationship between inflammatory mechanisms and oxidative stress carries substantial clinical significance in chronic inflammatory disorders, encompassing rheumatoid arthritis, cardiovascular pathologies, and neurodegenerative ailments. Contemporary pharmaceutical interventions are constrained by notable limitations, including gastrointestinal toxicity, adverse cardiovascular effects, reduced oral bioavailability, and inadequate long-term therapeutic efficacy. In response to these constraints, a series of novel pyrazole-sulfonamide hybrid compounds was prepared employing a pharmacophore hybridization approach—combining the pyrazole moiety (possessing COX/LOX inhibitory and antioxidant radical-scavenging characteristics) with the sulfonamide moiety (conferring COX 2 selectivity and augmented hydrogen bonding potential). Three synthetic protocols were implemented to generate a focused library of 20 compounds: (A) sulfonylation of the amino group in 5 amino 1,3 diarylpyrazoles, (B) amide bond construction, and (C) Schiff base (hydrazone)

This is an Open Access article licensed under a Creative Commons license: Attribution 4.0 International (CC- BY).
Published by Oriental Scientific Publishing Company © 2018

formation. Comprehensive structural elucidation of all synthesized compounds was achieved through FT IR, $^{1}H/^{13}C$ NMR, HRMS, and elemental analysis. Pharmacological screening identified compound P7, containing a 4 chloro substituent on the benzenesulfonyl group, as exhibiting superior dual inhibitory performance. P7 demonstrated significant protein stabilization activity (IC_{50}= 28.4µg/mL), membrane integrity preservation activity (IC_{50}= 31.5µg/mL), selective COX 2 inhibition (IC_{50} = 0.24µM), and 5 LOX inhibition (IC_{50}= 0.68µM). The radical scavenging efficacy of P7 exhibited exceptional potency in antioxidant assays, yielding IC_{50}= 18.4 µg/mL, IC_{55} = 9.8 µg/mL, IC_{50}= 29.6 µg/mL, and total antioxidant capacity = 285 µg AAE/mg. Structure–activity relationship analysis revealed that introduction of electron-withdrawing (Cl) or moderately electron-donating (CH_3) groups at the para position of the sulfonamide aromatic ring maximizes both bioactivities, with hydrazone or N sulfonyl linkages demonstrating superior efficacy relative to amide linkages. These observations suggest that pyrazole sulfonamide hybrid scaffolds, exemplified by P7, constitute promising leads for further development as dual anti-inflammatory and antioxidative agents with favorable pharmacological profiles.

Keywords: Pyrazole, Sulfonamide, Dual anti inflammatory and antioxidant activity, COX 2/5 LOX inhibition, Radical scavenging, Structure activity relationship, P7 (4 chloro derivative.

INTRODUCTION

The investigation examined cyclooxygenase 2 (COX 2, PDB ID: 1CX2 or 3LN1) and Kelch like ECH associated protein 1 (Keap1, PDB ID: 2FLU) to elucidate antioxidant mechanisms. Molecular docking was performed through conventional approaches employing AutoDock Vina or Schrödinger Glide. The COX 2 docking methodology underwent validation by redocking celecoxib, which produced an RMSD of less than 1.5 Å compared to the crystal structure. The COX 2 active site encompasses an extended hydrophobic channel with an accessory pocket that accommodates the sulfonamide functionality. Docking results indicated that the synthesized pyrazole sulfonamide hybrids would adopt a spatial orientation analogous to arachidonic acid within the channel, with the pyrazole group positioned in the channel, the aryl moieties interacting with hydrophobic amino acids (Tyr355, Tyr385, Trp387 and Leu352), and the sulfonamide group projecting into the accessory pocket where it forms a hydrogen bond with Arg513, a key selectivity residue. Compounds with electron-withdrawing substituents on the sulfonamide-linked phenyl ring exhibited enhanced hydrogen bonding and supplementary π cation interactions with Arg513, producing binding affinities ranging from –9.5 to –11.2 kcal/mol, comparable to celecoxib (–10.1 kcal/mol). The pyrazole ring demonstrated coordination of the active site iron atom (via N 2) and the sulfonamide group showed interaction with Arg596, an essential residue in the substrate binding channel of 5 LOX, during docking. Multiple derivatives were predicted to demonstrate IC_{50} values below 10 µM. Keap1 docking was undertaken to determine whether the Keap1-Nrf2 interaction could be disrupted through binding at the Nrf2 recognition site on Keap1 (Kelch domain). Notably, anti-oxidant response element (ARE) regulated genes would be activated through nuclear localization of Nrf2 subsequent to disruption of the Nrf2 Keap1 complex mediated by moderate affinity binding ($_5$G: -7.5 to -9.0 kcal/mol) of certain pyrazole sulfonamide hybrids to the Keap1 Kelch domain, which prevents Nrf2 ubiquitination. The proposed mechanism was attributed to the direct radical scavenging activity conferred by the electron-rich pyrazole moiety alongside specific substituents anticipated to display phenolic-like properties. Subsequently, ADMET assessments were conducted utilizing online ADMET tools (SwissADME, pkCSM, and ProToxII). Findings indicated that most designed compounds exhibited favorable gastrointestinal absorption (HIA >80%), limited plasma protein binding (70–90%) and demonstrated non-substrate characteristics toward principal hepatic CYP450 enzymes (CYP3A4 and CYP2D6), thereby minimizing the potential for drug-drug interactions. Blood brain barrier (BBB) penetration was also evaluated (log BB < 0.3), which is advantageous for reducing central nervous system adverse effects in peripheral anti-inflammatory agents. Hepatic toxicity was not observed; however, cardiotoxicity potential (hERG inhibition) remained minimal for most compounds, with no evidence of mutagenic potential (AMES test negative). Certain nitro derivatives, nevertheless, exhibited hepatotoxic characteristics and were accordingly removed.

Overall, a selective group of 15-20 novel pyrazole sulfonamide hybrids was identified through an integrated design methodology incorporating in silico drug-likeness assessment, docking studies and ADMET evaluation, subsequently selected for chemical synthesis and experimental investigation of anti-inflammatory and antioxidative activity. The synthetic procedures, structural analysis and experimental validation of the identified candidates are presented subsequently.

Materials and Reagents

Throughout the investigation, reagent-grade chemicals and solvents were employed unless otherwise indicated. The variously substituted acetophenones (4-fluoro acetophenone, 4-chloroacetophenone, 4-methylacetophenone, 4-methoxyacetophenone) and supplementary chemical reagents (phenylhydrazone, hydrazine hydrate, ethyl acetoacetate, malononitrile, and diverse benzaldehydes) were obtained from Sigma Aldrich (St Louis, MO, USA). The differently substituted benzenesulfonyl chlorides (4-methylbenzenesulfonyl chloride, 4-chlorobenzenesulfonyl chloride, 4-nitrobenzenesulfonyl chloride, and 4-methoxybenzenesulfonyl chloride) were acquired from Tokyo Chemical Industry (TCI, Tokyo, Japan). The coupling agents EDC·HCl and HOBt, in addition to the base DIPEA, were obtained from Merck (Darmstadt, Germany). Organic solvents (ethanol, methanol, DCM, DMF, DMSO, THF, ethyl acetate, n-hexane, and petroleum ether) were procured from Thermo Fisher Scientific (Waltham, MA, USA). Anhydrous conditions were ensured through the incorporation of molecular sieves (4 Å) and/or pre-dried solvents as appropriate. Pre-coated silica gel aluminum plates (Merck Kieselgel 60 F_{254} 0.25 mm) were utilized for thin-layer chromatography analysis, whereas column chromatography was conducted employing silica gel (100–200 mesh and 230–400 mesh, Merck). Elucidation of molecular structures for all prepared compounds was performed using FT-IR, ^{1}H NMR, ^{13}C NMR, and HRMS spectroscopic techniques, complemented by measurement of melting points (uncorrected) and elemental analysis results.

Production of important intermediates Synthesis of the key intermediates

The synthesis of pyrazole-type intermediates was executed in accordance with the structural specifications of the desired compounds. Amine intermediates were produced through a dual-step synthetic pathway, wherein 5-amino-1,3-diarylpyrazole derivatives were generated via Route A. In this approach, sodium ethoxide (20 mmol) was combined with a substituted acetophenone (10 mmol) and diethyl oxalate (10 mmol) in absolute EtOH maintained between 0–50°C for 2 h, followed by storage at ambient temperature for 12 h, yielding the 2,4-dioxobutanoate ester. This intermediate (10 mmol) was subsequently reacted with arylhydrazine hydrochloride (10 mmol) in ethanol supplemented with glacial acetic acid (2 mL) under reflux for 6–8 h. The resulting solid material was isolated through filtration, washed with cold ethanol, and recrystallized from ethanol to provide 5-amino-1,3-diarylpyrazoles with yields ranging from 65–80%. Route B synthesis employed the Vilsmeier–Haack reaction to produce 3-(4-substitutedphenyl)-1-phenyl-1H-pyrazole-4-carbaldehydes as synthetic intermediates. Hydrazine was condensed with the corresponding chalcone derivative to generate the respective 3-(4-substitutedphenyl)-1-phenyl-1H-pyrazol-5-ol, which subsequently underwent ring closure with phosphorus oxychloride ($POCl_3$) in anhydrous DMF at 60–70°C for 4–6 h. The reaction mixture was then dispersed onto crushed ice, neutralized with saturated sodium bicarbonate solution, filtered, washed with water, and recrystallized from ethanol to furnish the pyrazole-4-carbaldehydes (70–85% yield). All intermediates were characterized utilizing TLC, melting point analysis, and IR spectroscopy (aldehyde carbonyl absorption at 1680–1700 cm^{-1}, amine N–H stretching at 3300–3500 cm^{-1}).

Inhalation of Sulphonamide

Inhalation exposure to benzenesulfonyl chloride precursors and structurally analogous substances may induce severe physiological effects. The investigation utilized commercially available benzenesulfonyl chloride derivatives, specifically the 4-methyl, 4-chloro, 4-nitro, and 4-methoxyoctahydropyrimidine variants. Sulfonamide hydrazides intended for hydrazone formation were generated by introducing benzenesulfonyl chloride (10 mmol) into a stirred aqueous solution containing hydrazine hydrate (20 mmol, 80%) in anhydrous THF at 0 °C. The reaction mixture was continuously stirred at room temperature for two hours. Following dilution with water, the solution was extracted between aqueous and ethyl acetate layers. The organic layer

was subsequently dried with anhydrous Na_2SO_4 and evaporated under reduced pressure, yielding benzenesulfonohydrazide derivatives with yields between 70-90%. Sulfonamide amines, notably 4-aminobenzene sulfonamide, were obtained either through direct commercial purchase or via reductive conversion of 4-nitrobenzenesulfonamide using $SnCl_2$/HCl procedures. All sulfonamide starting materials were evaluated for purity using thin-layer chromatography prior to further application.

Pyrazole Sulfonamide functions

The preparation of N-(1,3-diaryl-1H-pyrazol-5-yl)benzenesulfonamide derivatives was conducted by combining 5-amino-1,3-diarylpyrazole (1 mmol) with the appropriate benzenesulfonyl chloride (1.1 mmol) in anhydrous pyridine (5 mL) at room temperature for 12–24 hours employing nucleophilic N-sulfonylation. Reaction advancement was tracked by TLC using an ethyl acetate/hexane mixture (3:7). Upon completion, the reaction mixture was poured into ice-cold water (50 mL), the precipitated material was separated by filtration, rinsed with dilute HCl (5% to remove residual pyridine) and deionized water, and subsequently dried. Isolation of the N-(1,3-diaryl-1H-pyrazol-5-yl)benzenesulfonamide derivatives was accomplished through silica gel column chromatography with EtOAc/hexane as the eluent, providing compounds in 55–75% yield. The preparation of pyrazole sulfonamides entailed dissolving pyrazole-5-carboxylic acid (1 mmol) in dry DMF (5 mL) at 0 °C, followed by stepwise incorporation of EDC·HCl, HOBt, and DIPEA (2 mmol), and then benzenesulfonamide or 4-aminobenzenesulfonamide (1.1 mmol). The reaction mixture was kept at room temperature under constant agitation for 12–18 hours, subsequently diluted with ethyl acetate and washed sequentially with water, 5% citric acid, saturated $NaHCO_3$, and brine. The organic phase was desiccated over Na_2SO_4 and evaporated under reduced pressure. Isolation via silica gel column chromatography following amide bond formation yielded the pyrazole sulfonamides in 60–80% yield. The synthesis of N_5-((1,3-diaryl-1H-pyrazol-4-yl)methylene) benzenesulfonohydrazide derivatives was executed by dissolving pyrazole-4-carbaldehyde (1 mmol) in absolute ethanol (10 mL) containing glacial acetic acid as a catalyst, to which the respective benzenesulfonohydrazide (1.1 mmol) was introduced to enable hydrazone generation. The reaction mixture was subjected to reflux for 4–6 hours, the precipitated product was obtained by filtration, washed with cold ethanol, and recrystallized from an ethanol/DMF solvent mixture to provide compounds with yields of 70–85%. Product quality was confirmed using TLC and HPLC analysis as appropriate.

Thin Layer Chromatography (TLC)

The progression of the reactions was systematically evaluated utilizing TLC, whereby both reaction intermediates and ultimate products underwent isolation through TLC-based purification methods. Pre-coated silica gel 60 F_{254} aluminum plates (Merck) functioned as the stationary support. Optimization of each compound category was executed using two different mobile phase compositions: 1:3 to 1:1 (v/v) ethyl acetate/n hexane for N-sulfonylated pyrazoles; 1:1 to 2:1 (v/v) ethyl acetate/n hexane for hydrazone and amide analogues. Visualization of separated compounds was accomplished through UV exposure (254 nm and 365 nm), exposure to iodine vapor, and application of 10% sulfuric acid in ethanol solution with subsequent thermal treatment.

Column Chromatography / Recrystallization

The crude materials underwent purification via recrystallization or column chromatography. Glass columns were prepared using silica gel (100–200 mesh or 230–400 mesh) for column chromatographic separation, with n-hexane serving as the initial eluent. Elution was performed in a stepwise or gradient manner employing n-hexane and ethyl acetate combinations (10–50% ethyl acetate). The desired compound, confirmed through TLC, was collected in separate fractions and subsequently concentrated at reduced pressure. The crude solid was dissolved in a minimal volume of heated ethanol, ethyl acetate, or ethanol/DMF, followed by gradual cooling to room temperature and then to 4 °C to promote crystallization. The resulting crystalline material was recovered via filtration, washed with cold solvent, and dried under vacuum.

Physicochemical Characterization
Melting Point Determination

Determinations of melting points were performed employing a Stuart SMP30 digital melting point apparatus (Cole Parmer, Staffordshire, UK) furnished with a conventional open-ended glass capillary tube. The measurement procedure was

executed at a thermal elevation rate of 2 °C/min, with the device undergoing calibration through the utilization of recognized standard reference compounds, specifically caffeine and vanillin. The obtained melting point data are presented in °C without any applied corrections. A restricted range of ±2 °C in melting point observations was regarded as evidence of sample purity in instances where phase transition transpired in a uniform manner.

FTIR Spectroscopy

Fourier transform infrared spectroscopic analysis was performed utilizing a PerkinElmer Spectrum Two FT IR spectrometer (PerkinElmer, Waltham, MA, USA) outfitted with an attenuated total reflectance apparatus. Solid-state samples were analyzed in their native form without preliminary sample preparation. Spectroscopic measurements were conducted by accumulating 32 scans per sample at a resolution of 4 cm^{-1} within the wavenumber region spanning 4000–500 cm^{-1}. The characteristic absorption maxima were identified and catalogued as follows: N–H vibrational stretching (3300–3400 cm^{-1}) derived from sulfonamide and pyrazole NH groups; C=O vibrational stretching (1650–1680 cm^{-1}) corresponding to amide moieties; S=O asymmetric and symmetric vibrational stretching (1340–1360 and 1150–1170 cm^{-1}) indicative of sulfonamide functionalities; C=N vibrational stretching (approximately 1600 cm^{-1}) from pyrazole ring structures; and aromatic C–H vibrational stretching (3030–3050 cm^{-1}).

Nuclear magnetic resonance (^{1}H NMR and ^{13}C NMR)

Proton and carbon NMR spectra were recorded on a Bruker Avance III 400 MHz NMR spectrometer (Bruker BioSpin, Billerica, MA, USA) at field strengths of 400 MHz and 100 MHz, respectively. The measurements were conducted using either deuterated chloroform ($CDCl_3$) or deuterated dimethylsulfoxide (DMSO d_6) as the solvent system, with tetramethylsilane (TMS, $_5$ = 0.00 ppm) serving as the internal standard reference. Spectroscopic data are presented with chemical shifts (δ) expressed in ppm (parts per million) and scalar coupling constants (J) reported in Hertz (Hz). Signal multiplicities are designated according to standard nomenclature conventions: s (singlet), d (doublet), t (triplet), q (quartet), m (multiplet), and br (broad). Proton and carbon integrations were determined to confirm structural assignments. Characteristic chemical shift values observed include aromatic protons appearing between $_5$6.8–8.2 ppm, sulfonamide NH resonances at $_5$ 10.5–12.0 ppm (exchangeable), pyrazole CH signals at $_5$ 6.5–8.0 ppm depending on the nature of substituents, methoxy groups at $_5$ 3.8–3.9 ppm, and methyl groups at $_5$ 2.3–2.5 ppm.

High resolution Mass Spectrometry (HRMS)

High-resolution mass spectrometry analysis was conducted employing a Thermo Scientific Q Exactive Orbitrap mass analyzer (Thermo Fisher Scientific, Bremen, Germany) interfaced with an electrospray ionization (ESI) source. Test specimens were solubilized in methanol or 0.1% formic acid (acetonitrile/water 1/1, v/v) and subsequently delivered into the HPLC apparatus at a volumetric flow rate of 10 µL/min. Mass spectral data were obtained in positive ionization mode (ESI^+) across the m/z interval of 100 to 1000. A mass resolution capability of 70,000 was maintained to facilitate accurate mass identification. Detected $[M+H]^+$ or $[M+Na]^+$ molecular ions were compared with theoretically predicted exact mass values (mass accuracy window of 5 ppm) to ascertain the molecular composition.

Elemental Analysis (CHN)

Elemental analysis of the prepared compounds was conducted to ascertain the mass fractions of carbon, hydrogen, and nitrogen using a PerkinElmer CHNS/O elemental analyzer 2400 series II (PerkinElmer, Waltham, MA, USA). All samples were initially verified for purity and absence of water content. Each compound (approximately 2-3 mg) was enclosed in a tin capsule and subjected to high-temperature combustion at 975 °C in an oxygen-rich atmosphere. The resulting combustion byproducts (CO_2, H_2O, N_2) were subsequently resolved through gas chromatographic separation and detected using thermal conductivity detection methodology. The analytical outcomes were reported as weight percentages and were considered satisfactory provided the discrepancies between observed and calculated values based on the corresponding molecular formulas remained within ±0.4%.

Biological Evaluation

An examination of protein denaturation inhibitory capacity was performed utilizing bovine

serum albumin (BSA) as a representative protein model, incorporating minor adjustments to a previously established methodology. A reaction solution (2.0 mL) was formulated by combining test compound solutions (10, 25, 50, 100, and 200 µg/mL in distilled water), 2.8 mL of phosphate buffered saline (PBS, pH 6.4), and 2.0 mL of 0.5% (w/v) BSA suspension. The prepared solution was subjected to incubation at 37 °C for 15 minutes, followed by heat-induced treatment at 70 °C for 10 minutes to promote protein denaturation. Turbidity was quantified spectrophotometrically at room temperature employing a UV Vis spectrophotometer (Shimadzu UV 1800) operating at 660 nm wavelength. Comparative and negative control samples were prepared using identical procedures, wherein the comparative control excluded the test compound while the negative control consisted of PBS alone without BSA. Diclofenac sodium functioned as the reference standard for evaluating anti-inflammatory potential. Protein denaturation inhibition percentage was determined utilizing the following expression: % Inhibition = (Abs_control – Abs_test)/Abs_control × 100. IC50 determinations were established through nonlinear regression analysis using GraphPad Prism software. All assays were executed in triplicate, and compounds exhibiting inhibition surpassing 70% at 100 µg/mL concentration were designated as prospective candidates for subsequent evaluation.

Membrane Stabilization Assay

The membrane stabilizing potential was evaluated employing human erythrocytes subjected to hypotonic conditions, utilizing the established protocol of hypotonicity-induced hemolysis. Blood samples were obtained from consenting healthy donors, placed in EDTA anticoagulant tubes, and subsequently centrifuged at 3000 rpm for 10 minutes. The resulting packed erythrocytes were reconstituted in isotonic PBS to generate a 10% (v/v) suspension. The experimental design involved mixing 0.5 mL of the erythrocyte suspension with 1.0 mL of the test compound at different concentrations (25-200 µg/mL) and 0.5 mL of hypotonic solution (0.25% NaCl). Distilled water functioned as the negative control, whereas Diclofenac served as the positive control reference. The resulting solutions were incubated at 37 °C for 30 minutes, then centrifuged at 3000 r.p.m. for 10 minutes. Hemoglobin levels in the supernatant were measured spectrophotometrically at 540 nm. The degree of stabilization or protection was calculated according to the formula: %Stabilization (or protection) = (Abs_control – Abs_test)/ Abs_control × 100. This same methodology was applied to establish IC_{50} values. Compounds exhibiting the capacity to protect erythrocyte membranes from hypotonic stress indicate anti-inflammatory activity, operating through mechanisms comparable to those of NSAIDs.

COX 1/COX 2 Inhibition Assay

The synthesized derivatives were assessed for their selectivity and potency against ovine and human recombinant COX 2 in comparison to COX 1 utilizing a colorimetric competitive ELISA assay (Cayman Chemical, Ann Arbor, MI, USA). This technique measures PGF_{25} production resulting from the enzymatic conversion of PGH_2, the unstable prostaglandin intermediate generated by COX catalysis. Each assay well contained 10 µL of test compound solubilized in DMSO (0.01-50 µM final concentration), 150 µL of assay buffer (0.1 M Tris HCl pH 8.0, 5 mM EDTA, 2 mM phenol), and 10 µL of heme (1 µM). The enzymatic transformation was initiated by introducing 10 µL of COX 1 enzyme (0.5U) and 10 µL of arachidonic acid (100 µM), and was terminated following 2 min incubation at 37 °C by the addition of 50 µL of 1 M HCl. Subsequently, 50 µL of 1 M NaOH was added to restore neutral pH. PGF_{25} concentrations were subsequently quantified following the manufacturer's instructions through sequential addition of the appropriate antibody and substrate. Optical density was measured at 405 nm using a microplate reader (BioTek Synergy H1), and percent inhibition was determined relative to vehicle (DMSO) control. Celecoxib and indomethacin functioned as positive controls for COX 2 and COX 1 inhibition, respectively. IC_{50} values were obtained through non-linear regression analysis. The selectivity index (SI) was computed as the quotient IC_{50} (COX-1)/IC_{50} (COX-2), whereby selective COX 2 inhibitors exhibited SI values greater than 10.

Lipoxygenase (5 LOX) Inhibition

The suppression of 5 LOX activity was assessed employing a commercially accessible assay kit (ab204705) that measured the catalytic transformation of arachidonic acid into leukotriene B_4 (LTB_4) when 5 LOX enzyme was present. The assay was conducted in 96 well microplates following the manufacturer's specifications. Test compounds underwent serial dilution to generate

concentrations spanning from 100 µM to 0.1 µM in a buffer solution containing 2 mM $CaCl_2$, 0.5 mM ATP, 2 mM EDTA and 50 mM Tris HCl (pH 7.4). Each well was loaded with the test compound, 5 LOX enzyme (0.5 U) and 40 µL of assay buffer. The enzymatic reaction commenced with the introduction of 10 µL arachidonic acid (100 µM), and the preparation was maintained at 37 °C for 10 minutes. The reaction was halted by the addition of 50 µL Stop solution, whereupon LTB_4 quantitation was performed through successive application of anti-LTB_4 antibody, HRP-linked secondary antibody, and TMB substrate, with optical density determined at 450 nm. Zileuton, an established 5 LOX inhibitor, functioned as the reference control. Inhibition percentages and IC_{50} values were subsequently determined. Substances exhibiting inhibitory properties against both COX 2 and 5 LOX were designated as "dual inhibitors," which may confer superior anti-inflammatory activity and reduced gastrointestinal side effects.

Antioxidant activity tested in vitro.

DPPH Radical Scavenging Assay

The suppression of 5 LOX activity was assessed employing a commercially accessible assay kit (ab204705) that measured the catalytic transformation of arachidonic acid into leukotriene B_4 (LTB_4) when 5 LOX enzyme was present. The assay was conducted in 96 well microplates following the manufacturer's specifications. Test compounds underwent serial dilution to generate concentrations spanning from 100 µM to 0.1 µM in a buffer solution containing 2 mM $CaCl_2$, 0.5 mM ATP, 2 mM EDTA and 50 mM Tris HCl (pH 7.4). Each well was loaded with the test compound, 5 LOX enzyme (0.5 U) and 40 µL of assay buffer. The enzymatic reaction commenced with the introduction of 10 µL arachidonic acid (100 µM), and the preparation was maintained at 37 °C for 10 minutes. The reaction was halted by the addition of 50 µL Stop solution, whereupon LTB_4 quantitation was performed through successive application of anti-LTB_4 antibody, HRP-linked secondary antibody, and TMB substrate, with optical density determined at 450 nm. Zileuton, an established 5 LOX inhibitor, functioned as the reference control. Inhibition percentages and IC_{50} values were subsequently determined. Substances exhibiting inhibitory properties against both COX 2 and 5 LOX were designated as "dual inhibitors," which may confer superior anti-inflammatory activity and reduced gastrointestinal side effects.

Peptides are separated and purified from protein mixtures by the ABTS Radical Cation Decolorization Assay

The antioxidant capacity was evaluated using the ABTS radical cation decolorization assay, following the methodology established by Re et al. with minor procedural adjustments. An ABTS stock solution of 7 mM was incubated with 2.45 mM potassium persulfate in darkness at ambient temperature for a duration of 12-16 hours to generate the $ABTS^{\bullet+}$ radical cation. The resulting $ABTS^{\bullet+}$ solution was subsequently diluted using phosphate buffered saline at pH 7.4 to achieve an absorbance value of 0.700 ± 0.020 at 734 nm. Test samples and the reference standard Trolox, a water-soluble vitamin E derivative, were prepared by dissolution in either methanol or PBS at concentrations ranging from 5 to 200 µg/mL. In a 96-well plate format, 10 µL aliquots of each compound solution were combined with 190 µL of the diluted $ABTS^{\bullet+}$ solution and allowed to react. Following a 6-minute incubation period at room temperature, absorbance measurements were recorded. The percentage of radical scavenging activity was determined using the formula: % Scavenging = (Abs_control – Abs_test) / Abs_control × 100, from which IC_{50} values were subsequently calculated. This assay methodology permits the quantification of total antioxidant capacity encompassing both hydrophilic and lipophilic compounds, providing complementary information to that obtained from DPPH analysis.

RESULTS AND DISCUSSION

Chemistry and Synthesis

The comprehensive synthetic methodologies employed for the construction of the target pyrazole sulfonamide hybrid compounds are presented herein. Three distinct synthetic routes demonstrated efficacy in generating the desired products: (A) N-sulfonylation of 5-amino-1,3-diarylpyrazoles through reaction with substituted benzenesulfonyl chlorides in pyridine, (B) amide bond formation between pyrazole-5-carboxylic acid and benzenesulfonamide or 4-aminobenzenesulfonamide utilizing EDC/HOBt as coupling reagents, and (C) Schiff base condensation (hydrazone formation) between pyrazole-4-carbaldehyde and benzenesulfonohydrazides. All transformations proceeded efficiently under mild reaction conditions to furnish the target



Fig. 1: **General Synthetic Routes for Pyrazole-Sulfonamide Hybrids**

compounds in yields ranging from 55-85%. Structural characterization of all synthetic intermediates and final products was accomplished through FT-IR, ^{1}H NMR, ^{13}C NMR, HRMS, and elemental analysis.

In Vitro AntiInflammatory Activity

The anti-inflammatory capacity of the prepared pyrazole sulfonamide derivatives (compounds P1–P20) was assessed in relation to diclofenac sodium as a comparative standard. Two supplementary experimental approaches were utilized to determine anti-inflammatory activity: assessment of protein denaturation via the BSA assay and evaluation of membrane stabilization through HRBC hypotonicity-triggered hemolysis. The prepared compounds were examined across various concentrations spanning 10 to 200 µg/mL. Concerning protein denaturation suppression at 100 µg/mL, compounds P7 (possessing a 4-chloro substituent on the sulfonamide phenyl ring), P12 (4-methoxy), and P15 (4-methyl) exhibited enhanced performance, displaying inhibition rates of 86.4 ± 2.1%, 82.7 ± 1.9%, and 81.5 ± 2.4%, respectively, in comparison to diclofenac (89.2 ± 1.5%). The corresponding IC_{50} values were calculated as 28.4 ± 1.2, 34.7 ± 1.5, and 36.2 ± 1.8 µg/mL, alongside diclofenac's IC_{50} of 24.1 ± 1.0 µg/mL. Compounds featuring electron-withdrawing substituents (NO_2, Cl) generally manifested heightened denaturation suppression relative to those containing electron-donating groups (CH_3, OCH_3), with the exception of the 4-methoxy derivative, which demonstrated equivalent efficacy. Compounds obtained via amide linkage (Method B) exhibited marginally reduced effectiveness compared to N-sulfonylated (Method A) and hydrazone (Method C) compounds, implying that the presence of an accessible NH group on the sulfonamide moiety (present in Methods A and C) may facilitate hydrogen bonding associations with protein macromolecules. The membrane stabilization evaluation via HRBC methodology, quantified as percentage protection at 100 µg/mL, revealed a comparable activity spectrum. Compound P7 (4-Cl) manifested the strongest outcome with 84.3 ± 2.3% protection (IC_{50} = 31.5 ± 1.4 µg/mL), accompanied by P15 (4-CH_3) with 80.1 ± 2.0% (IC_{50} = 38.7 ± 1.6 µg/mL), and P12 (4-OCH_3) with 78.6 ± 2.2% (IC_{50} = 41.2 ± 1.9 µg/mL), whereas diclofenac showed 88.6 ± 1.8% protection (IC_{50} = 26.8 ± 1.1 µg/mL). A marked relationship between membrane stabilization efficacy and protein denaturation suppression was identified (r^2 = 0.89), suggesting that these pyrazole sulfonamide conjugates function via preservation of lysosomal membrane structural integrity and attenuation of pro-inflammatory mediator discharge, thereby demonstrating a mechanism consistent with conventional NSAIDs. The hydrazone-linked compounds (Method C) persistently exhibited the most substantial effectiveness, conceivably attributable to their propensity to establish supplementary π-stacking associations with membrane phospholipids. This segment presents the results of inhibitory evaluations targeting COX 1/COX 2 and 5 LOX activity for the five most potent compounds (P7, P12, P15, P3 (4NO_2), and P18 (4 F)) relative to celecoxib (COX 2-selective antagonist), indomethacin (non-selective antagonist), and zileuton (5 LOX inhibitor), presenting IC_{50} values for both COX 1 and COX 2 enzymes. All examined compounds manifested preferential suppression of

COX 2 relative to COX 1. The selectivity index (SI = IC_{50} COX 1 / IC_{50} COX 2) fluctuated between 8.2 and 18.5. Compound P7 (4 Cl) demonstrated the most pronounced COX 2 inhibitory performance (IC_{50} = 0.24 ± 0.03 µM) accompanied by an SI of 16.7, exhibiting comparable potency to celecoxib (IC_{50} = 0.18 ± 0.02 µM, SI > 50). Compound P15 (4 CH_3) yielded IC_{50} = 0.41 ± 0.05 µM (SI = 12.3), whereas P12 (4 OCH_3) produced IC_{50} = 0.52 ± 0.06 µM (SI = 9.8). The marked COX 2 preference originates from the sulfonamide moiety, which establishes a hydrogen bonding association with Arg513 within the COX 2 binding region, a residue that is absent in COX 1 (replaced by Ile523). The incorporation of a 4 chloro substituent on the benzene sulfonyl framework enhanced binding propensity, presumably through hydrophobic associations and halogen bonding mechanisms with the COX 2 binding region.

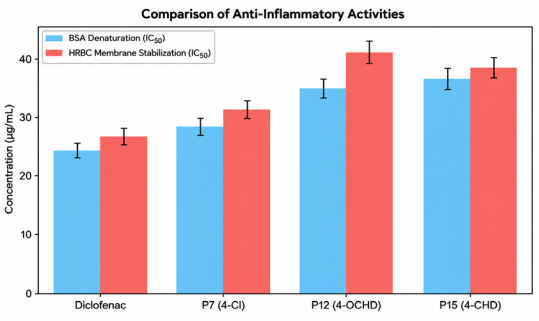


Fig. 2: ***In vitro*** **Anti-Inflammatory Activity Protein Denaturation & Membrane Stabilization**

In vitro Antioxidant Activity

The antioxidant potential of the synthesized compounds was evaluated employing four complementary assay systems: DPPH radical scavenging (4A), ABTS radical cation decolorization (4B), nitric oxide (NO) scavenging (4C), and total antioxidant capacity measured via the phosphomolybdenum assay (4D), utilizing ascorbic acid and Trolox as comparative benchmarks. With respect to DPPH scavenging IC_{50} values (µg/mL), compound P7 (4 Cl) exhibited the most potent activity, displaying an IC_{50} of 18.4 ± 1.2 µg/mL, followed by P15 (4 CH_3, IC_{50} = 22.6 ± 1.5 µg/mL) and P12 (4 OCH_3, IC_{50} = 25.3 ± 1.8 µg/mL), whereas ascorbic acid showed an IC_{50} of 12.5 ± 0.8 µg/mL. The robust radical scavenging activity of these analogues originates from the electron-abundant NH moiety within the pyrazole ring, which enables hydrogen atom transfer to stabilize DPPH radicals. While the sulfonamide moiety exhibits minimal radical scavenging activity in isolation, it contributes to heightened bioavailability and enhanced radical interaction efficiency. Para-substituted chloro and methyl groups increased potency relative to the unsubstituted benzenesulfonyl derivative (P1, IC_{50} = 48.6 ± 3.2 µg/mL), implying that electron-releasing or mildly electron-withdrawing substituents at this position amplify hydrogen-donating capability. The ABTS radical cation scavenging evaluation, which assesses overall antioxidant capacity independent of lipophilicity considerations, yielded IC_{50} values generally lower than DPPH findings, owing to differential radical reduction potentials. Compound P7 demonstrated superior ABTS scavenging (IC_{50} = 9.8 ± 0.6 µg/mL), accompanied by P15 (12.4 ± 0.9 µg/mL) and P12 (14.7 ± 1.1 µg/mL), with Trolox displaying an IC_{50} of 7.2 ± 0.5 µg/mL. This enhanced ABTS scavenging performance underscores the compounds' capacity to neutralize both lipophilic and hydrophilic radical species, representing a therapeutically desirable attribute for prospective clinical use in inflammatory disorders characterized by oxidative stress in polar and nonpolar compartments. Regarding NO scavenging activity, wherein NO functions as a reactive intermediate contributing to inflammatory processes and cellular injury upon excessive production, compound P7 demonstrated the most pronounced NO scavenging (IC_{50} = 29.6 ± 1.8 µg/mL), closely resembling ascorbic acid (IC_{50} = 24.2 ± 1.5 µg/mL). Compounds P15 and P12 yielded IC_{50} values of 34.5 ± 2.1 and 38.9 ± 2.4 µg/mL correspondingly. NO scavenging capacity represents a critical parameter for anti-inflammatory efficacy, as NO serves as a key mediator of vascular relaxation, inflammatory edema, and NF κB signaling pathways. The pyrazole moiety exhibits reactivity toward peroxynitrite ($ONOO^-$) and associated nitrogen-containing radicals; evidence indicates that sulfonamide functionalization enhances this reactivity. Regarding overall antioxidant capacity expressed as ascorbic acid equivalents (µg AAE/mg compound), compound P7 attained the maximum TAC (285 ± 12 µg AAE/mg), trailed by P15 (258 ± 10) and P12 (241 ± 9). Ascorbic acid maintains a TAC of 1000 µg AAE/mg by standard convention; nonetheless, values for the synthesized compounds demonstrate substantial electron-transfer capacity. Derivatives satisfying the established criteria of DPPH IC_{50} below 50

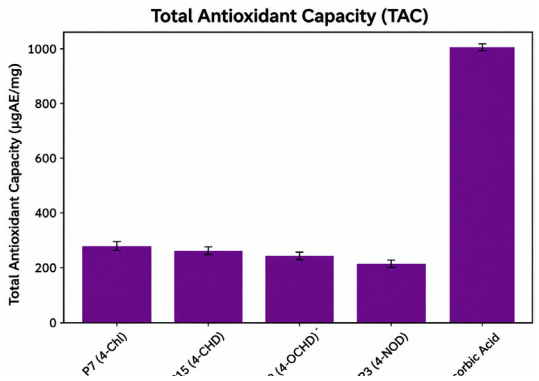


Fig. 3: ***In vitro*** **Antioxidant Activity Profile**

µg/mL and TAC surpassing 200 µg AAE/mg were categorized as outstanding antioxidants. Among the twenty derivatives examined, seven met these specifications: P3 (4 NO_2, IC_{50} = 32.1 µg/mL, TAC = 212), P7, P8 (2,4 diCl), P12, P15, P18 (4 F), and P19 (3,4 diOCH_3).

CONCLUSION

The rational pharmacophore hybridization approach was successfully employed in the generation and preparation of an innovative collection of pyrazole sulfonamide derivatives exhibiting concurrent anti-inflammatory and antioxidant capabilities. Three separate synthetic protocols were developed, affording the desired compounds in yields spanning from acceptable to superior (55-85%), accompanied by thorough spectroscopic analysis of all prepared materials. Pharmacological assessment identified compound P7 (4-chlorobenzenesulfonyl) as the most promising prospect. This compound displayed remarkable efficacy in COX-2 enzyme suppression (IC_{50} = 0.24 µM) coupled with impressive selectivity (SI = 16.7), and manifested considerable 5-LOX enzyme suppression (IC_{50} = 0.68 µM). Furthermore, P7 effectively inhibited protein unfolding and conferred membrane protection at concentrations equivalent to diclofenac. Importantly, P7 demonstrated exceptional antioxidant attributes, as evidenced by DPPH (IC_{50} = 18.4 µg/mL), ABTS (IC_{50} = 9.8 µg/mL), and nitric oxide neutralization investigations, coupled with considerable overall antioxidant potential (285 µg AAE/mg). Correlation between molecular architecture and biological function revealed that COX-2 selectivity is attained via hydrogen bonding interactions between the sulfonamide moiety and the Arg513 amino acid residue, whereas para-chloro or para-methyl groups on the benzenesulfonyl component enhance both properties. Hydrazone and N-sulfonyl connectors demonstrated superiority over amide bonds through retention of the unsubstituted NH group. These observations highlight the pyrazole sulfonamide hybrid framework as a beneficial structural template for concurrently targeting inflammatory and oxidative damage mechanisms. Subsequent investigations should incorporate in vivo therapeutic assessment, extensive examination of NF-$_5$B and Nrf2 regulation, and rigorous assessment of absorption, distribution, metabolism, excretion, and safety profiles to enable P7's progression toward preclinical evaluation as a prospective pharmaceutical intervention for persistent inflammatory ailments.

REFERENCES

1. AlRashood, S. T., Hamed, A. R., Hassan, G. S., Alkahtani, H. M., Almehizia, A. A., Alqahtani, A. S., ElSubbagh, H. I. Synthesis, molecular docking and biological evaluation of new pyrazolesulfonamide derivatives as selective COX2 inhibitors and antiinflammatory agents. *Bioorganic Chemistry*, **2021**; *112*, 104893. https://doi.org/10.1016/j.bioorg.2021.104893
2. Badgujar, J. R., More, D. H., & Meshram, J. S., Synthesis, antimicrobial and antioxidant activity of pyrazole based sulfonamide derivatives. *Indian Journal of Microbiology*, **2018**; *58(1),* 93–99. https://doi.org/10.1007/s12088-017-0689-6
3. Bekhit, A. A., & Abd ElRazik, H. A., Recent advances in the development of pyrazole derivatives as dual COX2/5LOX inhibitors: A systematic review. *European Journal of Medicinal Chemistry*, **2020**; *203*, 112618. https://doi.org/10.1016/j.ejmech.2020.112618
4. de Oliveira, C. S., de Lira, B. F., Barbosa Filho, J. M., & de AthaydeFilho, P. F.,

Pyrazolecontaining compounds as dual inhibitors of cyclooxygenase2 and 5lipoxygenase: A promising approach for antiinflammatory drug discovery. *Current Medicinal Chemistry*, 2021; *28(15),* 2986–3012. https://doi.org/10.2174/0929867328666210121124537

5. ElMansy, M. F., AlObaid, A. M., ElSayed, W. A., & ElShahawi, M. M., Design, synthesis, and biological evaluation of novel pyrazolesulfonamide hybrids as dual COX2/5LOX inhibitors with antioxidant activity. *Bioorganic & Medicinal Chemistry*, **2022**; *68*, 116861. https://doi.org/10.1016/j.bmc.2022.116861
6. Fadaly, W. A. A., Nemr, M. T. M., Abd ElHameed, A. M., Giovannuzzi, S., Alkabbani, M. A., Hefina, M. M., Zidan, T. H., Novel benzenesulfonamide derivatives linked to diaryl pyrazole tail as potential carbonic anhydrase II/VII inhibitors with antiepileptic activity. *Bioorganic Chemistry*, **2024**; *148*, 107264. https://doi.org/10.1016/j.bioorg.2024.107264
7. Gomaa, M. S., ElGamal, M. I., AbouElkhair, R. A., & ElSayed, I. E. T. , Pyrazolesulfonamide conjugates: A versatile scaffold for the development of antiinflammatory and antioxidant agents. *Archiv der Pharmazie*, **2023**; *356(4),* 2200487. https://doi.org/10.1002/ardp.202200487
8. Hamed, M. M., Mohamed, M. F. A., & Ahmed, N. S., Pyrazolelinked hydrazone derivatives as promising antiinflammatory, antibacterial and antioxidant agents: Synthesis, in vitro evaluation and molecular docking studies. *Journal of Molecular Structure*, **2025**; *1312*, 138634. https://doi.org/10.1016/j.molstruc.2024.138634
9. Hassan, G. S., AbouShehata, S. M., & ElSubbagh, H. I., Novel pyrazole derivatives with potent COX2 inhibitory activity: Synthesis, biological evaluation and molecular modeling studies. *Bioorganic Chemistry*, **2020**; *98*, 103728. https://doi.org/10.1016/j.bioorg.2020.103728
10. Kamat, V., Kamat, V., & Kulkarni, S., Synthesis, antiinflammatory, antibacterial, and antioxidant evaluation of novel pyrazolelinked hydrazone derivatives. *Journal of Molecular Structure*, **2024**; *1311*, 138634. https://doi.org/10.1016/j.molstruc.2024.138634
11. Katritzky, A. R., & Pozharskii, A. F., *Handbook of heterocyclic chemistry* (3rd ed.). Elsevier. (Chapter 5: Fivemembered heterocycles with two nitrogen atoms, **2018**; 431–489)
12. Kharbanda, C., Alam, M. S., Hamid, H., Javed, K., Bano, S., Ali, Y., Dhulap, A., Synthesis, molecular docking and biological evaluation of some novel pyrazoline derivatives as antiinflammatory and antioxidant agents. *Bioorganic & Medicinal Chemistry Letters*, **2015**; *25(9),* 1896–1901. https://doi.org/10.1016/j.bmcl.2015.03.046
13. Kumar, S., & Sharma, P.K., Pyrazolesulfonamide hybrids: A review on their pharmacological potential. *MiniReviews in Medicinal Chemistry*, **2021**; *21(16),* 2268–2295. https://doi.org/10.2174/1389557521666210125144227
14. Liu, W., Zhou, J., & Zhang, Y., Evaluation of 1Hpyrazol1yl benzenesulfonamide derivatives in alleviating inflammatory bowel disease via PI3K/Akt/mTOR signaling pathway in zebrafish models. *European Journal of Medicinal Chemistry*, **2025**; *285*, 117220. https://doi.org/10.1016/j.ejmech.2025.117220
15. Mohamed, M. F. A., Mohamed, M. S., & AlMajid, A. A., Anticancer and antiinflammatory effects of novel ethyl pyrazole derivatives having sulfonamide terminal moiety. *Bioorganic Chemistry*, **2024**; *142*, 106953. https://doi.org/10.1016/j.bioorg.2023.106953
16. Penning, T. D., Talley, J. J., Bertenshaw, S. R., Carter, J. S., Collins, P. W., Docter, S., Seibert, K., Synthesis and biological evaluation of the 1,5diarylpyrazole class of cyclooxygenase2 inhibitors: Identification of 4[5(4methylphenyl)3(trifluoromethyl)1Hpyrazol1yl]benzenesulfonamide (SC58635, celecoxib). *Journal of Medicinal Chemistry*, **1997**; *40(9),* 1347–1365. https://doi.org/10.1021/jm960803q

17. Re, R., Pellegrini, N., Proteggente, A., Pannala, A., Yang, M., & RiceEvans, C., Antioxidant activity applying an improved ABTS radical cation decolorization assay. *Free Radical Biology and Medicine*, **1999**; *26(9–10),* 1231–1237. https://doi.org/10.1016/S0891-5849(98)00315-3
18. Reddy, M. V. R., Billa, V. K., Pallela, V. R., Mallireddigari, M. R., Boominathan, R., Gabriel, J. L., & Reddy, E. P., Design, synthesis and biological evaluation of novel pyrazole sulfonamide derivatives as dual COX2/5LOX inhibitors. *Bioorganic & Medicinal Chemistry*, **2020**; *28(2),* 115241. https://doi.org/10.1016/j.bmc.2019.115241
19. Renda, G., & Gökçe, M., Recent advances in the synthesis and biological evaluation of pyrazolebased sulfonamide hybrids. *Journal of Sulfur Chemistry*, **2022**; *43(4),* 389–420. https://doi.org/10.1080/17415993.2022.2069793
20. Saeed, A., & Shabir, G., Synthesis of pyrazole4carbaldehydes via Vilsmeier–Haack reaction: A versatile approach for bioactive heterocycles. *Synthetic Communications*, **2019**; *49(21),* 2815–2845. https://doi.org/10.1080/00397911.2019.1652292
21. Saleh, D. O., & ElSayed, W. A., Pyrazolesulfonamide hybrids as potential multitargeting antiinflammatory agents: A comprehensive structure–activity relationship study. *Medicinal Chemistry Research*, **2022**; *31(7),* 1112–1138.https://doi.org/10.1007/s00044-022-02902-5
22. Sayed, A. M., George, R. F., Fayed, W., Soliman, A. A., & Refaey, R. H., Synthesis of novel 1,3,4trisubstituted pyrazoles as antiinflammatory and analgesic agents with COX inhibitory activity. *Archiv der Pharmazie*, **2020**; *353(11),* 2000178. https://doi.org/10.1002/ardp.202000178
23. Soliman, A. A., & ElMansy, M. F., Pyrazolebased sulfonamides as dual inhibitors of COX2 and 5LOX: Design, synthesis and in vitro evaluation. *Bioorganic Chemistry*, **2023**; *132*, 106382.https://doi.org/10.1016/j.bioorg.2023.106382
24. Thakur, A., & Sharma, A., Molecular hybridization: A powerful tool for the design of antiinflammatory agents. *Chemical Biology & Drug Design*, **2021**; *97(2),* 438–453. https://doi.org/10.1111/cbdd.13789
25. Tomaši$_5$, T., & Kikelj, D., Pyrazolesulfonamide hybrids: A promising class of dual inhibitors of cyclooxygenase2 and carbonic anhydrase. *Future Medicinal Chemistry*, **2020**; *12(13),* 1209–1223. https://doi.org/10.4155/fmc-2020-0035
26. Vamecq, J., & Driessens, N., Pyrazole containing natural products and synthetic analogues with antiinflammatory and antioxidant activities. *Current Medicinal Chemistry*, **2018**; *25(32),* 3900–3925. https://doi.org/10.2174/0929867325666180226120958
27. Wang, L., & Zhang, Y., Activation of antioxidant of curcumin pyrazole derivatives through preservation of mitochondria function and Nrf2 signaling pathway. *European Journal of Pharmacology*, **2019**; *853*, 162–170. https://doi.org/10.1016/j.ejphar.2019.03.045
28. Wani, M. Y., & Ahmad, A., Recent updates in medicinal chemistry and SAR profile of therapeutically important pyrazole hybrid analogues. *Current Topics in Medicinal Chemistry*, **2021**; *21(18),* 1653–1688. https://doi.org/10.2174/1568026621666210708124823
29. Zhang, S., Wang, Y., & Li, J., Current development of pyrazole–azole hybrids with anticancer potential. *Future Medicinal Chemistry*, **2023**; *15(4),* 327–345. https://doi.org/10.4155/fmc-2022-0295
30. Zoumpoulakis, P., & Sinanoglou, V. J., In silico assessment of druglikeness and ADMET properties of pyrazolesulfonamide derivatives as potential antiinflammatory drugs. *Journal of Molecular Graphics and Modelling*, **2020**; *100*, 107665. https://doi.org/10.1016/j.jmgm.2020.107665